PROCESS INTENSIFICATION FOR HYDROGEN PRODUCTION FROM AMMONIA

E.M. IZURIETA[†,‡], M.N. PEDERNERA[†,‡] and E. LÓPEZ[‡]

† *Departamento de Ingeniería Química, Universidad Nacional del Sur (UNS), Bahía Blanca, Argentina.*
‡ *Planta Piloto de Ingeniería Química – PLAPIQUI (Universidad Nacional del Sur – CONICET), Bahía Blanca, Argentina.*
eizurieta@plapiqui.edu.ar

***Abstract*— Ammonia is presented as one of the main carriers for the transport and storage of hydrogen under mild conditions. In this context, the present work introduces the integration and intensification of an ultrapure hydrogen production process from ammonia as a feedstock. A production scale is set to satisfy the requirements of a typical hydrogen refueling station (200 kg_{H2}/day). A multifunctional shell-and-tube reactor is designed to carry out the ammonia cracking reaction. The system operates at a moderate pressure (8 bar) and in a temperature range for the ammonia decomposition reaction between 300 °C and 650 °C. Total ammonia conversion is achieved due to the chemical equilibrium shift by H_2 extraction through the incorporation of 100 % selective membranes. The Pd-Ag membranes provide a recovery of about 86 % of the hydrogen produced. The remaining hydrogen (i.e., the non-permeated stream) is catalytically combusted representing the only source of heat of the entire process.**

***Keywords*— Hydrogen production; Process intensification; Ammonia cracking; Membrane reactor; Hydrogen fuel station.**

I. INTRODUCTION

For several decades, governments of industrialized nations have tried to implement energy policies which minimize the damages to the planet. A future associated with sustainable energy consumption is a fundamental part of the actual global debate on climate change due to carbon dioxide emissions, main greenhouse gas resulting from human activities. According to the Paris Agreement (United Nations, 2015), the average global temperature should be kept below 2°C above pre-industrial levels, with efforts to limit this increase to 1.5°C, recognizing that this would significantly reduce the risks and effects of climate change. The anthropogenic sources of greenhouse gases are numerous, from which a relevant portion corresponds to energy use (IAPG, 2017). In a planet powered by fossil fuels, activities such as transport, electricity generation, industry and residential comfort services contribute to emissions, which challenges the search for solutions to reduce them.

Nowadays, actions to reduce carbon dioxide emissions and guarantee energy supply include the minimization of fossil fuels consumption, the development of CO_2 capture technologies and the production of alternative energy from renewable sources (Bains *et al*., 2017; Franzitta *et al*., 2017). To this end, whether from an economic or political point of view, alternatives are sought in the short, medium and long term in technological developments that allow a restructuring of energy systems. In line with this approach, process intensification is one of the main strategies of chemical engineering to face the ever-increasing demands of designing and operating chemical industries as efficiently and sustainably as possible. This concept is based on the development of new equipment and techniques that lead to cleaner technologies, more efficient energy-use and with substantially smaller equipment (Stankiewicz and Moulijn, 2000). Therefore, processes intensification and new applications development require a significant improvement in the design and performance of reaction units. Multifunctional reactors (those that integrate multiple unit operations in a single equipment) are seen as an interesting alternative in the search to achieve the imposed environmental objectives.

Within this kind of reactors, a type of multifunctional equipment of growing interest is the membrane reactor. A membrane can be defined as an interface that separates two zones and/or acts as a barrier to the mass transport through it thanks to a driving force. The stream that leaves the system after having passed the membrane is called permeate, while the stream that is rejected by the membrane is called retentate. In these units, it is possible to combine the kinetic effect given by the catalyst and the separation effect provided by the membrane. The integration of the two operations in a single unit offers advantages not only in terms of equipment simplification (process intensification) but also introduces improvements in the selectivity and/or conversion of certain processes (Spallina *et al*., 2018). One of the main applications of membrane reactors aims to increase the conversion in equilibrium-limited reactions, displacing it by preferential permeation of some of the reaction products (Barbieri *et al*., 2001).

In addition, it is important to note that the use of membrane reactors would not only shift the chemical equilibrium in the ammonia decomposition reaction and improve the yield of the products by increasing the conversion, but could also avoid NH_3 emissions to the atmosphere due to its total consumption (<1800 μg/m³ in 8 hours at Buenos Aires province, Argentina (GPBA, 2018)) due to its total consumption. This fact appears technologically much more complex to achieve in conventional reactors without coupled permeation.

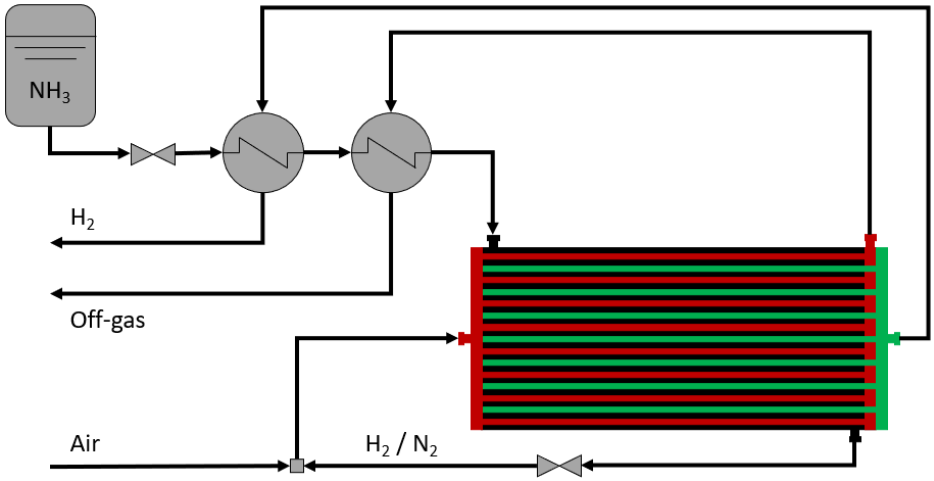

Figure 1: Flow diagram for the autothermal process of ammonia-fueled H_2 delivery station.

In the search for a harmonious diversification of these renewable sources for different sectors and at different scales, hydrogen is pointed out as a natural substitute for hydrocarbons. Hydrogen is a clean fuel, since its combustion only produces water vapor, avoiding the generation of carbon oxides. In addition, hydrogen, unlike heat and electricity, is a highly versatile energy vector that not only allows energy to be transported, but also to be stored efficiently. However, there is a debate about what would be the best storage alternatives (Moradi and Groth, 2019). Among the existing proposals, transport and storage as ammonia (-33 °C and 1 bar or 25 °C and 10 bar), to be reconverted into H_2 at the time of consumption appears among the most efficient compared to the transport of H_2 as compressed gas (typically at 350 bar or 700 bar), liquefied (at -253 °C), or by means of another hydrogenated carrier (for example, methanol) (Salmon and Bañares Alcántara, 2021).

The development of the infrastructure for hydrogen refueling stations is another fundamental point aiming the gradual replacement of traditional fuels. Some countries such as the United States or Germany project a strong growth in the number of retail vending stations and, in the near future, this trend should be replicated in the different signatory nations of the Paris Agreement in order to achieve the goals agreed.

According to the bibliography about current hydrogen refueling stations, the average installations are estimated with dispensing capacities in the range of 200 to 1600 kg_{H2}/day, the smallest being the most common (Reddi *et al*., 2017; USA Department of Energy, 2020). As an interesting alternative to the straightforward hydrogen storage as compressed gas or cryogenic liquid, this paper studies a process fed with ammonia as raw material. Ammonia can conveniently be stored at room temperature at relatively low pressures, to be converted into H_2 on-demand or stored in buffer containers during hours of low consumption. To this end, process intensification techniques are exploited to perform a reaction comprising high energy consumption and limited by chemical equilibrium.

II. METHODS

A. Process Description

An autothermal process for the production of ultrapure hydrogen from ammonia is proposed here, as shown in Fig. 1. Ammonia is stored in a tank as a liquid at its saturation pressure at room temperature (25 °C, ~10 bar). A decompression valve allows to regulate the pressure of the circuit downstream the storage tank. Subsequently, two heat exchangers in-series are employed to evaporate the NH_3 and to overheat the stream up to the reaction conditions.

The reactor of choice comprises a shell-and-tube design, in triangular arrangement. The shell (i.d.=33.33cm, L=1.0m) is packed with Ru-K/CaO catalytic pellets (Sayas *et al*., 2020) (1 mm-diameter, spherical) to carry out the ammonia cracking reaction (Eq. 1). Regarding the tubes, (i.d. = 8.0mm, o.d.=13.4 mm, all tubes), the bundle is divided into two different types. On one hand, 200 Pd-Ag based membrane tubes with a thickness (δ_M) of 25 µm and an infinite selectivity to hydrogen are arranged (green circuit in Fig. 1). On the other hand, the non-permeated fraction of the stream resulting from cracking (retentate stream, black circuit in Fig. 1) is mixed adiabatically with air (at 25 °C) and fed to the other type of tubes (100 units, red circuit in Fig. 1). In there, the catalytic combustion of the remaining hydrogen is conducted (Eq. 2) in order to generate the heat required for the endothermic cracking (Eq. 1). For this purpose, the inner wall of the tubes intended for combustion are washcoated with a 75µm-layer of Pd/Al_2O_3 catalyst (Gritsch, 2008).

$$NH_3 \leftrightarrow 1.5\ H_2 + 0.5\ N_2 \qquad \Delta H_1^\circ = 45.9\ kJ/mol \qquad (1)$$

$$H_2 + 0.5\ O_2 \rightarrow H_2O \qquad \Delta H_2^\circ = -241.8\ kJ/mol \qquad (2)$$

The outlet streams from both groups of tubes (i.e., combustion exhaust gases and permeated ultrapure hydrogen) are used as hot streams in the heat exchangers, with the dual purpose of evaporating/preheating ammonia and recovering the calorific value of the process output streams.

The operating pressure of the ammonia cracking process was arbitrarily fixed at 8 bar, seeking a balance between two opposing phenomena. On one hand, hydrogen permeation through the membrane is controlled by the

difference of hydrogen partial pressures at both sides of the membrane, which acts as the driving force for the separation process. In these terms, higher pressures favor the H_2 purification. On the other hand, the equilibrium conversion of the ammonia cracking reaction is enhanced by operating at lower pressures (as dictated by Le Châtelier's law)

Ammonia flowrate was set at 0.9 mol_{NH3}/s (1322 kg/day) with the goal of achieving a production of 200 kg_{H2}/day net. According to Eq. 1, this flowrate would generate a higher H_2 production than the target (at complete ammonia conversion and hydrogen recovery). Nevertheless, as mentioned above, part of the H_2 generated must be used (through its catalytic combustion) to satisfy the energy balance of the whole process.

B. Mathematical model

The multifunctional reactor under study was represented by means of a steady state pseudo-homogeneous one-dimensional mathematical model. In addition, isobaric operation was assumed, with no heat loss to the environment, uniform flow distribution in the tubes, and negligible homogeneous reactions. The equations which describe the model are the following:

Ammonia cracking stream:

$$\frac{dF_{NH_3,1}}{dz} = A_{T1} \cdot (-r_1 \cdot \rho_B) \quad (3)$$

$$\frac{dF_{H_2,1}}{dz} = A_{T1} \cdot (1.5 \cdot r_1 \cdot \rho_B) - \sigma_{t3} \cdot J_{H_2} \quad (4)$$

$$\sum_i \left(F_{i,1} \cdot C_{P\,i,1}\right) \cdot \frac{dT_1}{dz} = A_{T,1} \cdot r_1 \cdot (-\Delta H_1) - \sigma_{t2} \cdot U_{12} \cdot (T_1 - T_2) - \sigma_{t3} \cdot U_{13} \cdot (T_1 - T_3) \quad (5)$$

Hydrogen combustion stream:

$$\frac{dF_{H_2,2}}{dz} = \sigma_{t2} \cdot (-r_2) \quad (6)$$

$$\sum_i \left(F_{i,2} \cdot C_{P\,i,2}\right) \cdot \frac{dT_2}{dz} = \sigma_{t2} \cdot r_2 \cdot (-\Delta H_2) + \sigma_{t2} \cdot U_{12} \cdot (T_1 - T_2) \quad (7)$$

Permeated hydrogen stream:

$$\frac{dF_{H_2,3}}{dz} = \sigma_{t3} \cdot J_{H_2} \quad (8)$$

$$F_{H_2,3} \cdot C_{P\,H_2,3} \cdot \frac{dT_3}{dz} = \sigma_{t3} \cdot \left(J_{H_2} \cdot C_{P\,H_2,3} + U_{13}\right) \cdot (T_1 - T_3) \quad (9)$$

Reaction rates:

$$r_1 = k_1^{\circ} \cdot \exp\left(-\frac{Ea_1}{R \cdot T_1}\right) \cdot \frac{p_{NH_3}^{0.5}}{p_{H_2}^{1.9}} \cdot \left(1 - \left(\frac{p_{N_2} \cdot p_{H_2}^3}{K_{eq} \cdot p_{NH_3}^2}\right)\right) \quad (10)$$

$$r_2 = k_2^{\circ} \cdot \exp\left(-\frac{Ea_2}{R \cdot T_2}\right) \cdot p_{H_2} \quad (11)$$

Permeated hydrogen flux:

$$J_{H_2} = \frac{Q_0}{\delta_M} \cdot \exp\left(-\frac{Ea_M}{R \cdot T_1}\right) \cdot \left(p_{H_2,1}^{0.5} - p_{H_2,2}^{0.5}\right) \quad (12)$$

In Eqs. 3 to 12, $F_{i,j}$ represents the molar flowrate of each species (i = NH_3, H_2, N_2, O_2, H_2O) in each stream (j = 1: cracking, 2: combustion, 3: permeate), z is the axial coordinate of the reactor, A_T is the cross-sectional area, σ_t is the total perimeter of the tubes assigned to each combustion or permeate section (number of tubes per diameter of each tube) and T_j is the temperature of each stream. U_{12} and U_{13} are the global heat transfer coefficients between two sections (1-2: cracking and permeate, and 1-3: cracking and combustion) according to Leva's correlations (Froment *et al*., 2011), J_{H2} is the hydrogen flux permeated through the membrane according to the Sievert's law with permeation parameters (Q_0 and Ea_M) as reported by Barbieri *et al*. (Adrover *et al*., 2017), r_j is the reaction rate (Eq. 1: cracking (Sayas *et al*., 2020), Eq. 2: combustion (Gritsch, 2008)), $C_{P\,i,j}$ the heat capacity of each species (Yaws, 1999) and ρ_B is the bed density. The equilibrium constant of the cracking reaction was obtained following the guidelines described by Elliott and Lira (2012). Selected parameters are reported in Table 1.

Table 1. Permeation and reaction parameters

Permeation parameters [a]
$Q_0 = 7.7 \cdot 10^{-5}$ mol/(s·m·atm$^{0.5}$)
Ea_M = 16 300 J/mol
Ammonia cracking parameters [b]
k_1° = 8584.8 (mol·atm$^{-1.4}$)/(s·g_{cat})
Ea_1 = 111 000 J/mol
Hydrogen combustion parameters [c]
k_2° = 130 000 mol/(s·m²·bar)
Ea_2 = 41 570 J/mol

a: (Adrover *et al*., 2017)
b: (Sayas *et al*., 2020)
c: (Gritsch, 2008)

The simulation of the process flow diagram presented in Fig. 1 was carried out in the gPROMS 4.0 environment (Siemens Process Systems Engineering, 2022). The differential equations of the multifunctional reactor were discretized using a second-order central finite difference method. The heat exchangers, mixer and decompression valve were solved through mass and energy balances, considering each unit as adiabatic. From the resolution of the presented system of equations, the axial temperature and concentration profiles were obtained for each of the reactor streams, as well as the outlet conditions of the heat exchangers, the valve and the mixer. A limit range of 300 C to 650 C was imposed for the temperature of the cracking and permeate streams to ensure the integrity of the Pd-Ag membranes.

III. RESULTS

A. Results on the process simulation

Figure 2 presents axial profiles of the molar flowrates (F) for each species in the reactor. Figure 2A reports flowrates corresponding to the compounds in the ammonia cracking stream and, additionally, the H_2 flowrate inside the membrane tubes (i.e., the permeate stream, green line). Fig. 2B shows flowrates for the components in the combustion tubes (N_2 is omitted aiming an improved visualization of the results). Complementary, Figure 3 reports axial temperature profiles for each stream within the reactor. It should be noted that the temperature of the feed to the combustion tubes is calculated from the adiabatic mixing of the air stream at room temperature (25 °C), with the outlet stream from the cracking zone at 607 °C (containing the non-permeated H_2).

According to the results presented in Figs. 2A and 2B, a steep drop in NH_3 flowrate is observed in the inlet region, with a conversion accounting 15 % in the first

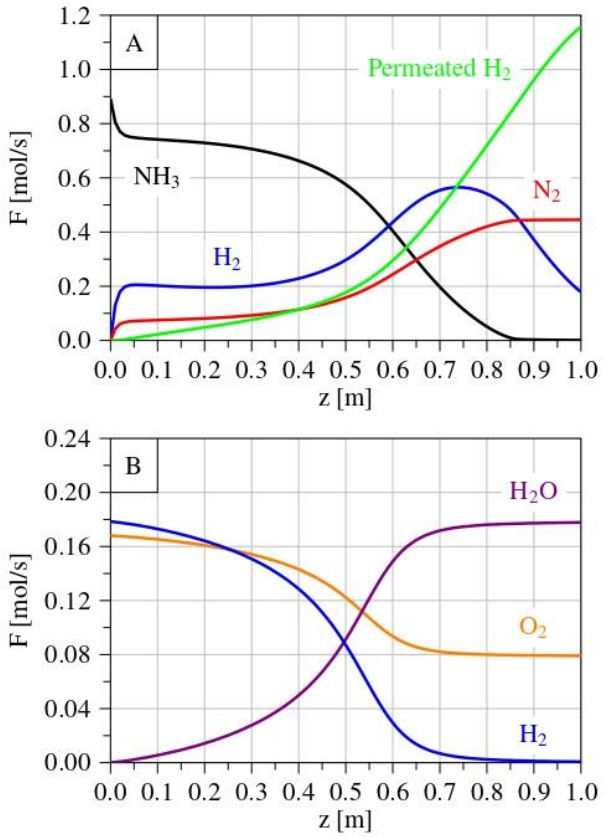

Figure 2: Axial molar flowrate profiles in (A) ammonia cracking section and hydrogen permeate tubes and (B) hydrogen combustion tubes (N_2 omitted).

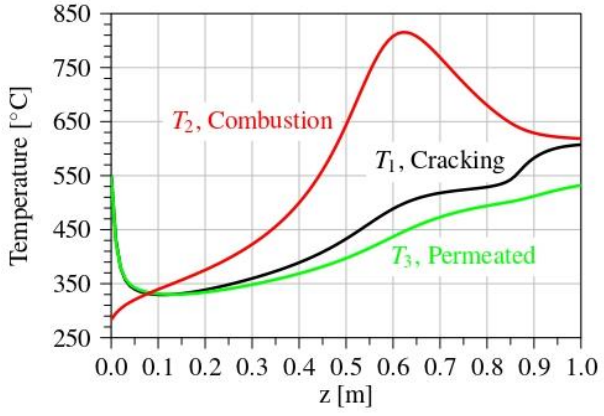

Figure 3: Axial temperature profiles.

0.03 m. Then, it slows down to convert 20 % of the ammonia near the first quarter of the unit. From there, the reaction turns on again. Finally, in an axial position of approximately 0.85 m, the ammonia concentration is already reduced to traces. This behavior segmented into zones agrees with the thermal level throughout the reactor (Fig 3). Thus, in the first zone, the high inlet temperature along with a high NH_3 partial pressure lead to a high reaction rate and a quasi-adiabatic behavior is observed. In fact, in this inlet zone, the reaction endothermicity leads to a strong drop in temperature, reaching a minimum of 329 C. This low thermal level, in addition to the appearance of hydrogen, leads to a strong decrease in the reaction rate (see Eq. 10) that is reflected in the plateau zone of the NH_3 profile (Fig. 2A, $0.05 < z < 0.25$). After the first 0.08 m, the temperature of the combustion stream is already above that corresponding to the cracking section, delivering heat to the reaction side. From an axial position of 0.25 m, the cracking reaction ignites again, now up to consuming all the remaining ammonia. The temperature in the combustion stream achieves a maximum of 815 °C at $z \sim 0.62$ m, where the conversion of the hydrogen fuel is approximately 90 % (see Fig 2B). Further on the heat generated by the combustion reaction drastically decreases.NH_3 conversion at this point amounts ca. 60 % and the heat consumption product of the cracking reaction remains significant up to $z \sim 85$ m where, as mentioned, ammonia is reduced to traces. From that point forward, the thermal level equilibrates to its final temperature of 620 °C.

The possibility of achieving a complete conversion of ammonia is due to the shift in chemical equilibrium provoked by H_2 permeation. It is important to clarify that, in the absence of permeation, the conversion of NH_3 would reach a value close to 99 % at the reactor outlet temperature. Although this conversion is very high, prohibitive ammonia effluents would pose a considerable problem to address (loss of process performance, implementation of a recycle, postcombustion, etc.).

The axial profiles of hydrogen and nitrogen in the cracking stream show, in the first zone, the expected evolution according to the stoichiometry of the cracking reaction (see Fig 2A). However, the permeation process through the membrane leads to the appearance of a maximum in the profile of hydrogen flowrate of approximately 0.565 mol/s at $z = 74$ m. Further on, the H_2 flowrate drops to an outlet value of 0.179 mol/s, with the permeate flowrate achieving 1.157 mol/s of pure H_2. This performance represents a recovery of 86.64 % of the generated hydrogen and a net production of 200 kg_{H2}/day, i.e., the required target.

It should be noted that the combustion of the non-permeate H_2 (retained in the output cracking stream) is the only source of heat for the whole process, as shown in Fig. 2B. In this Figure, it can be seen that hydrogen combusts all along the reactor, reaching complete conversion near the reactor outlet. This effect appears favorable in order to get a distributed heat generation in the axial coordinate since a rapid combustion rate may generate hotspots and damage the reactor's materials. This controlled reaction rate is achieved due to the fact that the combustion catalyst is washcoated over the internal wall of the combustion tubes instead of using a catalytic packed bed. According to the scheme proposed in Fig. 1, the process succeeds in achieving the required energy integration. The combustion stream exiting the tubes at 618.6 C, has enough calorific value to conduct the preheating of the NH_3 stream from its saturation condition, ~18 C, up to the aimed temperature to enter the reactor (550 C). Downstream the heat exchanger, the flue gases leave the process at approximately 110 C. On the other hand, the output ultrapure H_2 stream at 532.2°C is used for the ammonia evaporation (originally stored as a liquid) in the

first heat exchanger, leaving the process at 27 C. As previously stated, the calorific value of the outlet stream from the cracking zone is used to preheat the inlet stream to the combustion tubes (up to 283.4 C), after its adiabatic mixing with air at room temperature.

B. Decoupling the separation effect as an example of a wrong design

Up to this point, the feasibility of implementing a process design in which ultrapure hydrogen is obtained altogether with the thermal integration and total NH_3 depletion is proved. As seen, the thermal coupling of reactions and membrane reactors are both promising alternatives for achieving multifunctionality in chemical reactors seeking the best alternatives for process intensification. As a result of this integration, not only equipment compactness is obtained but also an improvement in the performance towards the desired product is achieved (Izurieta *et al*., 2019).

However, regarding the process scheme presented here (with simultaneous coupling of reaction, thermal management and separation), special attention must be paid in terms of selecting appropriate design parameters. If not, the reactor could operate under a decoupled condition, which implies a decrease in efficiency, generation of hot/cold-spots, reduction in reactant conversion, etc.

To exemplify this unwanted situation, a study on parametric sensibility was performed and the main results are discussed. In this study, the membrane thickness, δ_M, is selected as variable, ranging from 25 to 50 μm (values usually reported in the open literature). In all cases, a production of 200 kg_{H2}/day is still aimed. The impact of δ_M on both the reactor length required to meet the production target and the length required to achieve 99 % ammonia conversion is analyzed. The maximum temperature in the combustion zone is also monitored. The correspondent results are exposed in Fig. 4 and 5.

Figure 4 shows both the required reactor length for achieving the goal hydrogen production and the axial position at which ammonia conversion reaches 99 %. This study exhibits the strong increment (~40 %) in the reactor length required to fulfill the target of 200 kg_{H2}/day by the sole implementation of membrane tubes with a thicker Pd-Ag layer (δ_M from 25 to 50 μm). Conversely, the reactor length required for ammonia depletion remains almost constant (~4 %) along the investigated thickness range, decoupling reaction and permeation phenomena as if they were two independent process units (in-series).

The small increment in the required length for 99 % ammonia conversion is also due to the lower permeation rates. Hydrogen inhibits the reaction rate slowing down the NH_3 conversion. This effect implies also a drop in heat consumption and, consequently, the magnitude of the hot-spot evolves. However, this increase is not severe (6.2 C in the whole range, as shown in Fig. 5), and leads to a slight shift in the position of the maximum towards the entrance (-1.5 cm, not shown). These results highlight the decoupling effect; the reaction section remains almost constant while the permeation zone moves downstream and acts as an independent unit. This clarifies the need of a detailed design in terms of selecting the reactor parameters to achieve an enhanced operation.

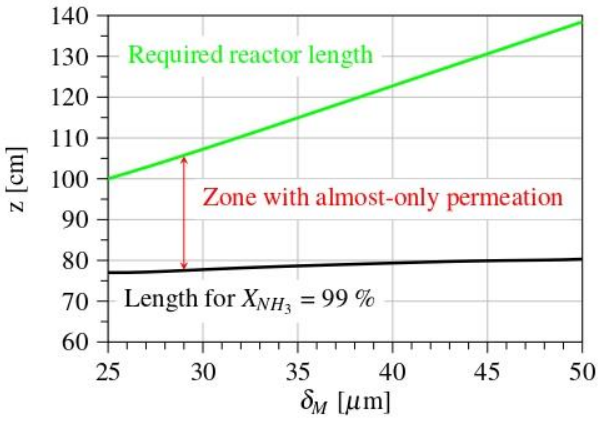

Figure 4: Required reactor lengths to achieve the hydrogen production goal (green) and 99 % ammonia conversion (black) for different membrane thicknesses.

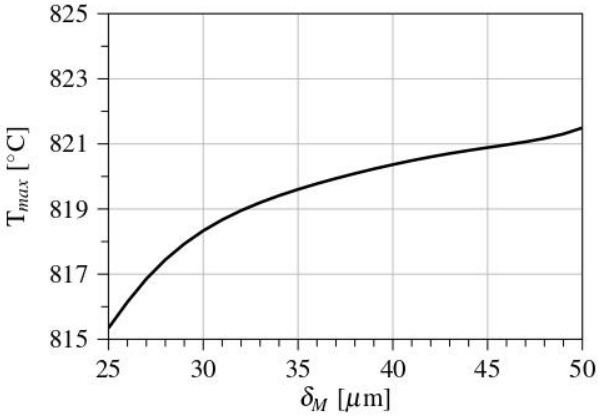

Figure 5: Maximum temperature at combustion section for different membrane thicknesses.

V. CONCLUSIONS

This work introduces a design proposal for a process aiming the intensification of the ultrapure hydrogen production from ammonia at the scales required by hydrogen refueling stations. A multifunctional shell-and-tube reactor is designed and dimensioned for a net production of 200 kg_{H2}/day. The NH_3 decomposition reaction was carried out at moderate pressure (8 bar) and in a temperature range that satisfies the limits imposed by Pd-Ag H_2 purification membranes. The proposed process achieves total conversion of NH_3 due to the hydrogen permeation through the membrane, which contributes to the chemical equilibrium displacement. In addition, the pure H_2 recovery reaches ca. 87 % from the total production via NH_3 cracking, while the remaining hydrogen is profited as the only source of heat for the entire process through catalytic combustion after mixing with atmospheric air.

In addition, a parametric sensibility analysis was performed in order to exemplify the need of a careful optimization of the design parameters. Wrong process intensification can lead to systems in which the selection of some parameters may imply much bigger units or less efficient processes. As shown here, a variation from 25 to

50 μm in the thickness of the Pd-Ag layer of the membrane leads to an increment of up to 40 % of the required reactor length. This not only translate to a higher cost of the process due to the higher volume, but also to a higher cost of the membrane itself since both the length and the thickness increase significantly.

ACKNOWLEDGES

The authors acknowledge the financial support by Consejo Nacional de Investigaciones Científicas y Técnicas (CONICET), Universidad Nacional del Sur (UNS), and Agencia Nacional de Promoción Científica y Tecnológica (ANPCyT).

REFERENCES

Adrover, M.E., Borio, D.O. and Pedernera, M.N. (2017) Comparison between WGS membrane reactors operating with and without sweep gas: Limiting conditions for co-current flow. *Int. J. Hydrogen Energy.* **42**, 5139–5149.

Bains, P., Psarras, P. and Wilcox, J. (2017) CO_2 capture from the industry sector. *Prog. Energy Combust. Sci.* **63**, 146–172.

Barbieri, G., Marigliano, G., Perri, G. and Drioli, E. (2001) Conversion-temperature diagram for a palladium membrane reactor. Analysis of an endothermic reaction: Methane steam reforming. *Ind. Eng. Chem. Res.* **40**, 2017–2026.

Elliott, J.R. and Lira, C.T. (2012) *Introductory chemical engineering thermodynamics*. Prentice Hall, Upper Saddle River, USA.

Franzitta, V., Curto, D., Milone, D. and Trapanese, M. (2017) Energy saving in public transport using renewable energy. *Sustainability*. **9(106)**, 1–19.

Froment, G.F., Bischoff, K.B. and De Wilde, J. (2011) *Chemical reactor analysis and design*. John Wiley & Sons, Hoboken, USA.

Gritsch, A. (2008) *Wärmeintegrierte Reaktorkonzepte für katalytische Hochtemperatur-Synthesen am Beispiel der dezentralen Dampfreformierung von Methan*. Ph.D Thesis, Universität Stuttgart, Germany.

GPBA (2018) *Decreto 2018 1074*. Buenos Aires Province Government).

IAPG (2017) *Energía, ambiente y mitigación de emisiones de CO_2*. Instituto Argentino del Petróleo y del Gas.

Izurieta, E.M., Pedernera, M.N. and López, E. (2019) Study of a thermally integrated parallel plates reactor for hydrogen production. *Chem. Eng. Sci.* **196**, 344–353.

Moradi, R. and Groth, K.M. (2019) Hydrogen storage and delivery: Review of the state of the art technologies and risk and reliability analysis. *Int. J. Hydrogen Energy*. **44**, 12254–12269.

Reddi, K., Elgowainy, A., Rustagi, N. and Gupta, E (2017) Impact of hydrogen refueling configurations and market parameters on the refueling cost of hydrogen. *Int. J. Hydrogen Energy*. **42**, 21855–21865.

Salmon, N. and Bañares Alcántara, R. (2021) Green ammonia as a spatial energy vector: A review. *Sustain. Energy Fuels*. **5**, 2814–2839.

Sayas, S., Morlanés, N., Katikaneni, S.P., Harale, A., Solami, B. and Gascon, J. (2020) High pressure ammonia decomposition on Ru-K/CaO catalysts. *Catal. Sci. Technol.* **10**, 5027–5035.

Siemens Process Systems Enterprise (2022) *gProms*. https://www.psenterprise.com/products/gproms

Spallina V., Matturro G., Ruocco C., Meloni E., Palma V., Fernandez E., Melendez J., Pacheco Tanaka D.A., Viviente Sole J.L., van Sint Annaland M., Gallucci F. (2018) Direct route from ethanol to pure hydrogen through autothermal reforming in a membrane reactor: Experimental demonstration, reactor modelling and design. *Energy*. **143,** 666–681.

Stankiewicz, A.I. and Moulijn, J.A. (2000) Process intensification: Transforming chemical engineering. *Chem. Eng. Prog.* **96**, 22–34.

United Nations (2015) *Paris Agreement*.

USA (2020) *Hydrogen fueling stations cost*. Department of Energy.

Yaws, C.L. (1999) *Chemical properties handbook*. McGraw-Hill, New York, USA.

Received: June 23, 2022
Sent to Subject Editor: August 1, 2022
Accepted: October 4, 2022
Recommended by Subject Editor Laura Briand